Experimental Investigation of Eutectic Formation in Cr coated Accident Tolerant Fuel Cladding and its Safety Implications

Boyeon Kweon, Hyunwoo Yook, Youho Lee*
Department of Nuclear Eng., Seoul National Univ., Gwanak-ro 1, Gwanak-gu, Seoul 08826, Republic of Korea
**Corresponding author: leeyouho@snu.ac.kr*

***Keywords :** Accident tolerant fuel, Zirconium, Eutectic, Steam oxidation, Diffusion.

1. Introduction

Zirconium(Zr) alloys have been utilized as materials for nuclear fuel cladding tubes for a long time due to their excellent mechanical properties and low neutron-absorption cross-section. However, Zr alloy cladding undergoes rapid oxidation and embrittlement under high-temperature steam oxidation conditions, resulting in the rapid generation of large amounts of hydrogen. This issue has emerged as a significant issue since the Fukushima nuclear disaster. Consequently, there has been a growing need for Accident Tolerant Fuel (ATF) that can significantly reduce steam oxidation and hydrogen generation rates during design-basis accidents (DBA) such as loss-of-coolant accidents (LOCA). Moreover, active research has been conducted to develop ATF that can maintain integrity without melting or collapsing even at temperatures higher than current safety regulatory limits.

ATF can be broadly categorized into concepts involving coating high oxidation-resistant materials onto the surface of existing Zr alloy cladding and the fabrication of cladding using entirely new materials. In the case of Zr alloy cladding coated with oxidation-resistant materials such as chromium(Cr), the use of proven materials allows for relatively quick implementation through empirical experimentation and computational modeling of newly added factors. Therefore, it is feasible to apply these coated cladding to existing reactors within a relatively short timeframe. Cr-coated claddings, a leading concept in coated cladding technology, are undergoing validation tests in reactors and are the focus of extensive research as one of the most promising ATF concepts both domestically and internationally.

From the perspective of nuclear fuel cladding safety regulation, the factor requiring new consideration for Cr-coated ATF compared to conventional ATF is the Zr-Cr eutectic reaction. Even with Cr coating, from the standpoint of normal operation and DBA, it is generally considered that ductility reduction due to inner wall oxidation resulting from cladding burst is the most limiting safety phenomenon. However, in scenarios Beyond DBA (BDBA), the melting points of Zr and Cr, ordinarily high at 1855 ℃ and 1907 ℃, respectively, decrease to 1332 ℃, significantly heightening the risk of structural collapse of the cladding due to Zr-Cr eutectic reactions, which becomes a critical concern.

Therefore, this study evaluated the risk of structural collapse of the cladding material due to the Zr-Cr eutectic reactions by confirming the oxidation and diffusion behavior of the cladding material at temperatures exceeding the eutectic onset temperature. Additionally, safety evaluations resulting from this phenomenon were conducted.

2. Experimental setup

Cr-coated Zr cladding (Zr-1.1Nb Alloy) was subjected to experiments in three different experimental setups and environments to investigate the behavior of the cladding due to the Zr-Cr eutectic reactions when exposed to temperatures above the onset temperature of 1308 ℃ [1].

Firstly, experiments were conducted to confirm the loss of protectiveness of Cr coating and the degradation and embrittlement behavior due to the eutectic reactions in a steam oxidation environment, and the risk of structural collapse of cladding under long-term exposure time was evaluated. The behavior in oxygen-free environments was also compared and validated through experiments. Finally, the cladding behavior under real-scale, with a focus not on the size of coupons or specimens, but rather on the actual scale was investigated.

2.1 Eutectic formation in steam oxidizing environment

To investigate the behavior of the Zr-Cr eutectic reaction in a high-temperature steam environment, a LOCA simulation facility was utilized. A schematic diagram of the LOCA simulation facility established at Seoul National University (SNU) is depicted in Fig. 1. (a). Cladding specimens with various Cr coating thicknesses (5, 8, 10, 12, 16 μm) and lengths of 8 mm were placed in a holder and introduced into the high-temperature steam furnace. The temperature inside the furnace was set above the onset temperature of the eutectic reaction, and the temperature profile of the specimens measured during the experiment is shown in Fig. 1. (b).

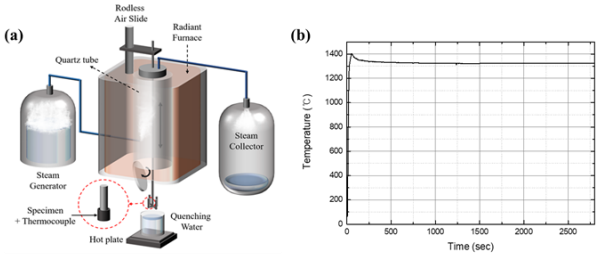

Fig. 1. (a) Schematic diagram of the LOCA simulated facility [2], (b) temperature profile of the specimens.

After exposure to the high-temperature steam environment above the onset temperature of the eutectic reaction for the target duration, the specimens were cooled in ambient air. Subsequently, the microstructure of each specimen was analyzed by scanning electron microscope (SEM) and electron probe microanalysis (EPMA).

2.2 Eutectic formation in an inert environment

The Zr-Cr eutectic reaction, excluding the influence of oxygen, was observed using a Differential Scanning Calorimeter (DSC). The experiment was conducted in a 99.9999% Argonne environment, and vacuum purging was conducted five times with oxygen trapping systems to minimize oxidation reaction during the experiment. The cladding tubes with 16 μm Cr coating were cut into 4 mm (L) x 4 mm (W) x 0.5 mm (D), and the inner surface of the cladding was mechanically polished to achieve a uniform and flat contact area with the sensor of the DSC equipment. The specimens for the eutectic reaction experiments in an inert atmosphere were heated to 1325 ℃ at a rate of 20 ℃/min and then subjected to an isothermal exposure time of 1 hour. Similarly, after the completion of the experiment, the microstructure of the specimens was analyzed using SEM and EPMA.

2.3 Eutectic formation during integral LOCA progression in real-scale fuel rods

Experiments in sections *2.1* and *2.2* utilized small specimens tailored to the characteristics of the experimental setup, making it challenging to observe the eutectic reaction of real-scale rods. Furthermore, during LOCA occurrences, nuclear fuel cladding undergoes a phenomenon known as ballooning and burst, where the cladding swells dramatically and eventually ruptures. In areas where a burst occurs, bilateral oxidation takes place. However, in regions far from the burst site, oxygen diffusion is impeded by the inserted fuel pellet, leading to one-sided oxidation that is relatively less influenced by oxygen. Therefore, experiments were conducted at a real-scale to examine the behavior of cladding due to oxidation and eutectic reactions resulting from ballooning and burst on a meter-scale.

The real-scale experiments on eutectic, ballooning, burst, and oxidation were conducted using the facility(*i*-LOCA) established at SNU depicted in Fig. 2. (a). One meter of test cladding rods coated with 15 μm Cr on Zr-1.1Nb Alloy were employed, and Cylindrical (D= 8.192 mm) ZrO_2 pellets were inserted into the rod, with the cold void volume of the rod set to 30cm^3 for the test. After sintering ZrO_2 pellets, they were pressurized to 5 MPa and heated under an Ar atmosphere using induction heating. The temperature profile at the center of the cladding is depicted in Fig. 2. (b).

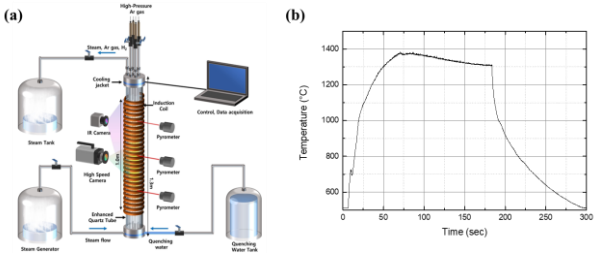

Fig. 2. (a) Schematic diagram of *i*-LOCA facility [3], (b) temperature profile of the specimen rod.

After exposure to a temperature exceeding the onset temperature of the eutectic reaction for the target duration (3 min), the specimen is cooled in ambient air.

3. Results and Discussion

3.1 Eutectic and oxidation in a steam environment

Through the Zr-Cr eutectic reactions and oxidation in a steam environment using the LOCA simulated facility, microstructural changes in the Zr-Cr-O system were observed at temperatures exceeding the onset temperature of the eutectic reaction.

Changes in the appearance of the specimens over oxidation time can be observed in Fig. 3. Results from exposure of the specimens for up to 2 hours indicate that the Cr-coated cladding undergoes significant embrittlement due to the oxidation but does not collapse due to the Zr-Cr eutectic reactions.

Fig. 3. Specimens shape over oxidation time

The changes in cross-sectional microstructure over time due to the Zr-Cr eutectic reaction and oxidation were observed using SEM and EPMA. Subsequently, a schematic diagram of the mechanism of cladding microstructure change due to oxidation above the eutectic onset temperature was completed. Fig. 4. and 5.

show the steps of the actual microstructure images and schematic diagrams that correspond to each other.

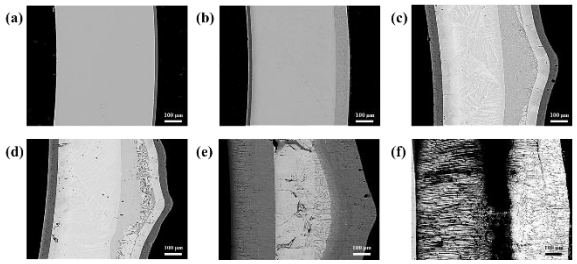

Fig. 4. SEM-BSE images of the cross-sectional evolution of Cr-coated ATF cladding due to the Zr-Cr eutectic and oxidation.

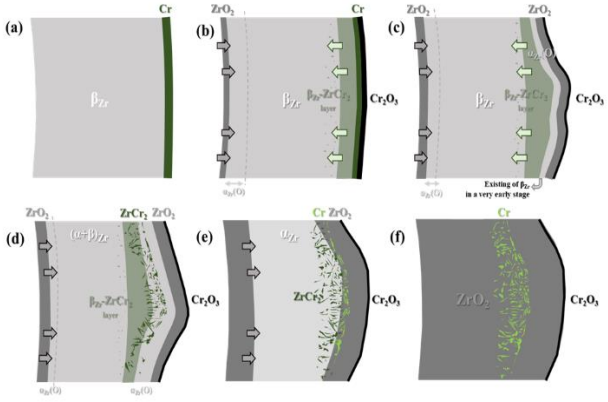

Fig. 5. Schematic diagram of the mechanism of cladding microstructure change due to oxidation above the eutectic onset temperature.

(a) in Fig. 4. and 5. illustrates the appearance of the specimen before the onset of eutectic reaction. Cr is uniformly coated on the surface of the cladding, and there is no diffusion of Cr into the Zr matrix during the coating process.

(b) in Fig. 4. and 5. depicts the stage where the Zr-Cr eutectic reaction begins (with residual oxidation resistance in the coating layer). In the case of the 16um Cr-coated cladding used in this study, the eutectic reaction commenced after approximately 20 seconds of exposure. Locally, the eutectic reaction initiates, and the eutectic phase (β-Zr+$ZrCr_2$ layer) formed by the reaction between $ZrCr_2$ and β-Zr penetrates inward into the β-Zr [4], as shown in Fig. 6.

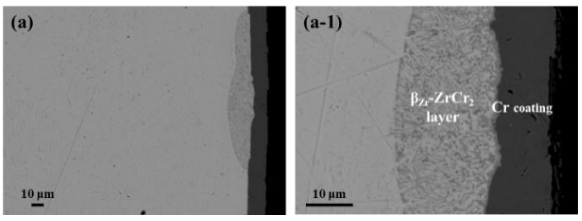

Fig. 6. BSE image of the specimen at the onset stage of the eutectic reaction. (a) x500, (a-1) x2.0k.

The eutectic phase that is locally formed gradually diffuses linearly into the Zr matrix over time, consuming the coating layer (Cr). At this stage, since the Cr coating layer still exists on the outer surface, outer wall oxidation does not occur. EPMA measurements of the Cr concentration in the eutectic phase revealed that the average Cr concentration was constant at approximately 15 wt.% regardless of the increase in eutectic phase thickness.

(c) in Fig. 4. and 5. depicts the stage where the coating loses its oxidation resistance, and outer wall oxidation begins. As the eutectic phase continues to consume the Cr coating layer spread inward into the Zr matrix, it eventually moves inward even after all Cr coating has been consumed. Consequently, β-Zr is exposed between the eutectic phase and the outer surface, and oxygen supplied along the grain boundaries of Cr_2O_3 formed on the coating layer surface leads to the formation of α-Zr, as shown in Fig. 7.

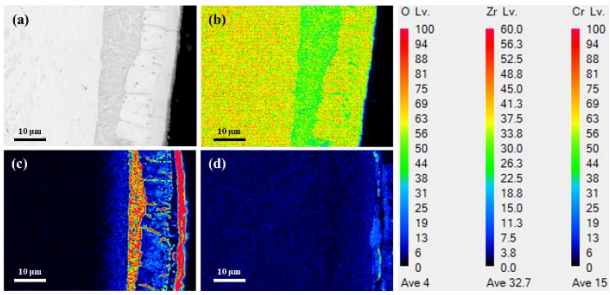

Fig. 7. EPMA element mapping data of specimen lost oxidation resistance due to the Zr-Cr eutectic reactions (a) BSE, (b) Zr, (c)Cr, (d) O.

By continuous exposure to high-temperature steam, oxidation progresses, leading to the formation of a ZrO_2 layer on the outer surface, and ongoing bilateral oxidation occurs. After the onset of bilateral oxidation, the linearly distributed eutectic phase begins to gather into a protruding shape (Fig. 4. (c)). This phenomenon is known to be associated with localized expansion related to the capillary effect of the liquid eutectic phase and solid-liquid volume changes [4]. The thickened eutectic phase will be referred to as the 'thick zone'.

After observing the microstructural changes over time, it was observed that the eutectic phase, which had been continuously moving into the Zr matrix direction, ceased its movement at a certain point (Fig. 4., 5. (d)). The reason for the cessation of movement of the eutectic phase is explained through Fig. 8.

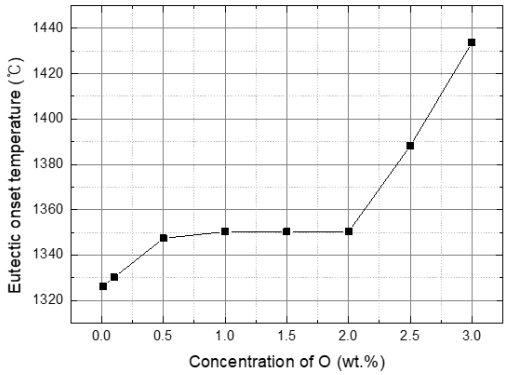

Fig. 8. Changes in the eutectic onset temperature with oxygen concentration in the Zr-Cr-O system.

Fig. 8. represents the results obtained from Thermo-Calc, showing the variation of the Zr-Cr-O eutectic onset temperature with the oxygen concentration in the Zr-Cr-O system. As the oxygen concentration increases, the Zr-Cr eutectic onset temperature, or melting point, rises with a steeper slope. In other words, the movement and cessation of the eutectic phase occur due to the increased Zr-Cr eutectic onset temperature caused by the elevated oxygen concentration.

In Fig. 4., 5. (f), as outer wall oxidation progresses, the α-Zr, which had formed between the Cr_2O_3 and the eutectic layer, oxidizes to ZrO_2, and oxygen is supplied to $ZrCr_2$, causing Cr reduction, as shown in Fig. 9. [5].

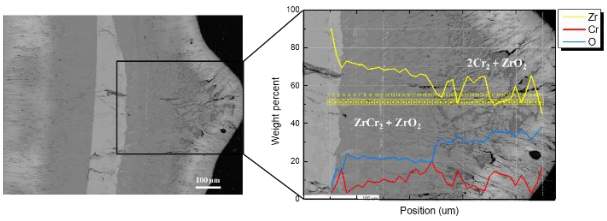

Fig. 9. EPMA element quantitative analysis data of Cr reduced from the $ZrCr_2$ layer within the ZrO_2 layer.

Due to the oxygen supplied from both outer and inner walls, all of the Zr matrix oxidizes to exist as the ZrO_2 phase (Fig. 4., 5. (f).

3.2 Safety margin assessment for structural collapse of cladding due to eutectic formation

In section *3.1*, it was confirmed that the cladding with the currently considered coating thickness, intended for commercial use, does not experience collapse even when exposed to prolonged periods in high-temperature steam environments above the Zr-Cr eutectic onset temperature. However, the phenomenon of cladding melting due to eutectic reactions still poses a critical threat to the integrity of coated claddings. Particularly, the accumulation of a 'thick zone' of the eutectic phase, especially if the coating thickness increases, may induce partial structural collapse of the cladding.

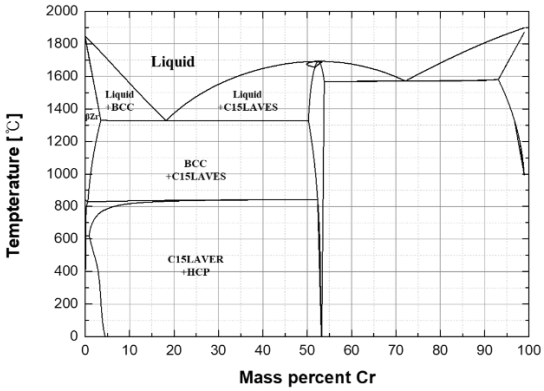

Fig. 10. Calculated Zr-Cr phase diagram using ThermoCalc software and TCZR1 database

As mentioned earlier, the Cr concentration of Zr-Cr eutectic phase analyzed through EPMA quantitative analysis is constant at about 15wt.%. This can theoretically be confirmed to be slightly lower than the Cr concentration of the eutectic phase, 18.17wt.%, which can be seen through the Zr-Cr binary phase diagram(Fig. 10.). Based on this experimental information, a simple, yet effective, model that predicts the maximum eutectic phase thickness with respect to initial coating thickness was proposed and experimentally validated to assess safety margin for the structural collapse of nuclear fuel rods with Zr-Cr eutectic reaction.

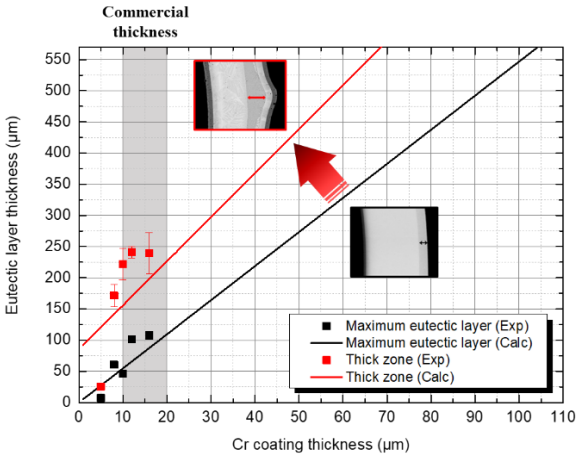

Fig. 11. Maximum eutectic phase thickness concerning coating thickness, considering the 'thick zone' factor.

According to the calculations, a Cr coating thickness of approximately 105 μm, which is about 10 times thicker than the currently considered commercialization, is necessary to generate the Zr-Cr eutectic phase thickness equivalent to the cladding (i.e., 570 μm), leading to structural collapse. To apply the 'Thick zone' factor, experiments were conducted with claddings of various coating thicknesses.

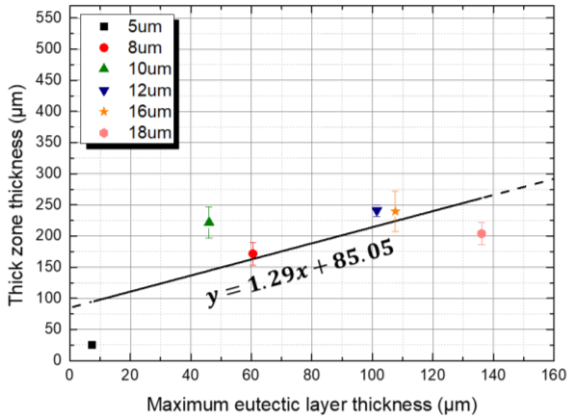

Fig. 12. Thick zone (Thick zone factor) by maximum eutectic layer.

Fig. 12. is a graph showing the thickness of the thick zone generated compared to the maximum eutectic thickness obtained through the experiment and a trend line obtained from the data. Considering the 'thick zone' factor, Cr coatings thicker than approximately 70 μm could result in the partial collapse of the fuel cladding geometry(Fig. 11.).

There are no reported instances regarding the eutectic phase's thickness that causes the cladding's collapse. However, even if not the entire cladding, situations where more than half of the thickness is covered by the eutectic layer could potentially compromise the structural integrity of the cladding. Therefore, it is deemed necessary to consider a Cr coating of approximately 20 μm thickness or more, taking into account the risk possibility.

3.3 Eutectic in an inert environment

The EPMA data of the ATF with a 16 μm–thick Cr coating exposed to 1 hour of isothermal exposure at 1325 ℃ in an inert environment is shown in Fig. 13.

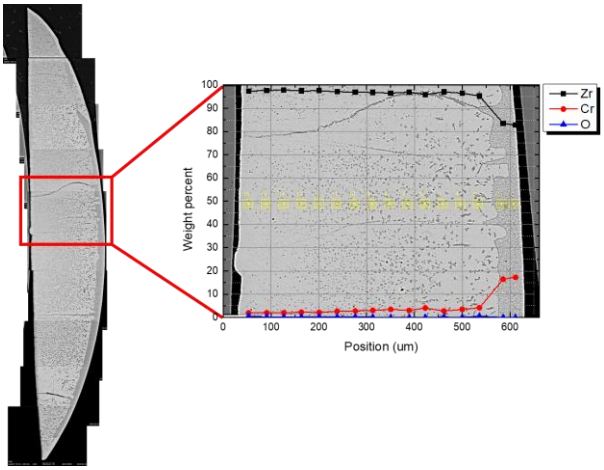

Fig. 13. SEM-BSE image of the DSC test specimen and EPMA element quantitative analysis data.

Through EPMA elemental quantitative analysis, it was confirmed that no oxidation had occurred. The Cr concentration within the eutectic phase was measured at 16.87 wt.%, similar to that observed in a steam environment. With no influence from oxygen, the eutectic phase, free from the oxidation effect, was found to be distributed throughout the entire Zr matrix.

3.4 Eutectic, ballooning, burst, and oxidation in real-scale

The distinct difference in the Zr–Cr eutectic reaction caused by oxygen in the burst region is evident in Fig. 14, which results from experiments with the *i*-LOCA facility.

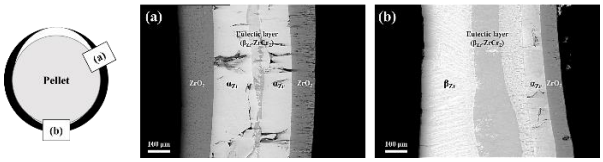

Fig. 14. SEM-BSE images of various circumferential orientations of the eutectic layer in the burst region.

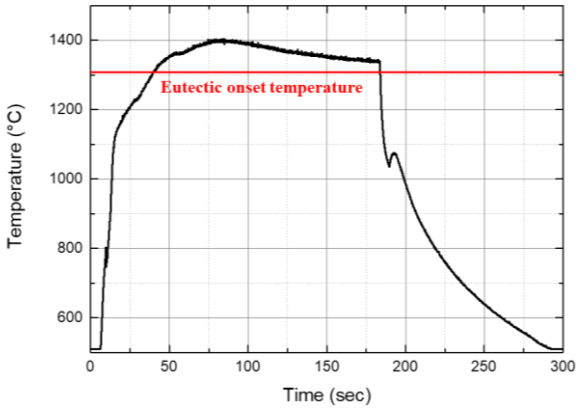

Fig. 15. Burst region temperature profile of i-LOCA experiment

In Fig.14., different circumferential orientations of the burst region are depicted. (a) shows the presence of bilateral oxidation due to a burst, where oxygen supplied from both the inner and outer walls causes the eutectic phase to be located at the center of the Zr matrix. Conversely, in (b), despite being a burst region, the supply of oxygen is impeded by ZrO_2 cylindrical pellets inserted inside the cladding rod, preventing inner oxidation while allowing outer oxidation. Consequently, the eutectic phase expands further towards the inside of the Zr matrix. As can be seen in Fig. 15, this is the difference in the eutectic reaction due to the influence of only oxygen experienced at the same temperature above the eutectic onset temperature.

Moreover, the tendency for the cross-section to become thicker and thinner along the length of the

cladding rod due to the Zr-Cr eutectic reaction was observed in the meter-scale experiments (Fig. 16.)

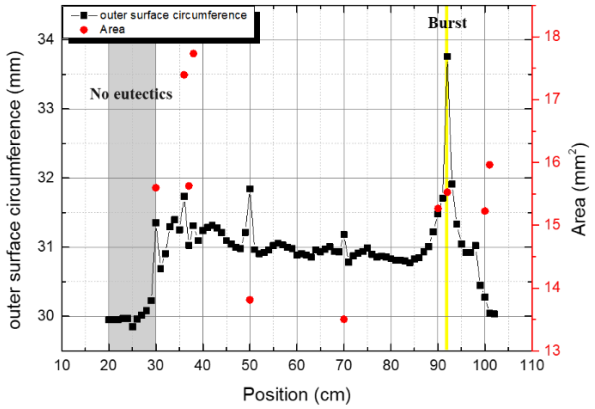

Fig. 16. Outer surface circumference and cross-sectional area of *i*-LOCA eutectic testing rod by length.

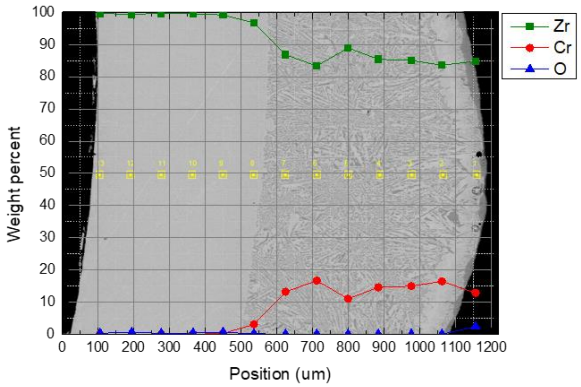

Fig. 17. EPMA element quantitative analysis data of *i*-LOCA experiment specimen where the thickness increased due to the Zr-Cr eutectic reaction.

The microscopic structure observed at the largest cross-sectional area, located at 36 cm in Fig. 16., is depicted in Fig. 17. The accumulation of the eutectic phase, flowed by the Zr-Cr eutectic reaction, results in a cladding thickness exceeding 1 mm, and the elemental concentration within the eutectic phase remained constant. This indicates the loss of cladding material due to the eutectic reaction in a relatively small area in Fig. 16(i.e., 50, 70 cm).

4. Summary and Conclusion

The structural collapse risk of the cladding material due to the Zr-Cr eutectic reaction has been evaluated. The Zr cladding with the Cr coating thickness under consideration for commercialization was found to withstand exposure to steam environments above the eutectic reaction temperature for up to 2 hours without structural collapse, although it undergoes significant embrittlement. The Zr-Cr eutectic phase tends to diffuse within the Zr matrix due to oxygen supplied from both inner and outer oxidation. A Cr coating with a thickness of approximately 105 μm is expected to ensure the structural collapse of the fuel rod, while a coating thickness of around 70 μm is anticipated to result in the partial collapse of the fuel cladding geometry due to the presence of a ‘thick zone’.

Acknowledgements

This work was supported by the Nuclear Safety Research Program through the Korea Foundation Of Nuclear Safety(KoFONS) using the financial resource granted by the Nuclear Safety and Security Commission(NSSC) of the Republic of Korea. (No. 00241683)

REFERENCES

[1] Kim, Dongju, Martin Ševeček, and Youho Lee. "Characterization of eutectic reaction of Cr and Cr/CrN coated zircaloy accident tolerant fuel cladding." Nuclear Engineering and Technology (2023).
[2] Joung, SungHoon, et al. "Post-quench ductility limits of coated ATF with various zirconium-based alloys and coating designs." Journal of Nuclear Materials 591 (2024): 154915.
[3] Yook, Hyunwoo, et al. " Integral LOCA experiment to study FFRD phenomena of high burnup ATF clad fuels." Korean Nuclear Society Spring Meeting. 2023.
[4] Brachet, Jean-Christophe, et al. "High temperature steam oxidation of chromium-coated zirconium-based alloys: Kinetics and process." Corrosion Science 167 (2020): 108537.
[5] Han, Xiaochun, et al. "An interesting oxidation phenomenon of Cr coatings on Zry-4 substrates in high temperature steam environment." Corrosion Science 156 (2019): 117-124.